Journal of Physics D:
Applied Physics

PAPER • **OPEN ACCESS**

Model of non-equilibrium near-cathode plasma layers for simulation of ignition of high-pressure arcs on cold refractory cathodes

To cite this article: D F N Santos *et al* 2024 *J. Phys. D: Appl. Phys.* **57** 405202

OPEN ACCESS
IOP Publishing
Journal of Physics D: Applied Physics
J. Phys. D: Appl. Phys. **57** (2024) 405202 (9pp)
https://doi.org/10.1088/1361-6463/ad5f3c

Model of non-equilibrium near-cathode plasma layers for simulation of ignition of high-pressure arcs on cold refractory cathodes

D F N Santos[1,2], **N A Almeida**[1,2], **L G Benilova**[1] and **M S Benilov**[1,2,*]

[1] Departamento de Física, Faculdade de Ciências Exatas e da Engenharia, Universidade da Madeira, 9000 Funchal, Portugal
[2] Instituto de Plasmas e Fusão Nuclear, Instituto Superior Técnico, Universidade de Lisboa, 1049-001 Lisbon, Portugal

E-mail: benilov@staff.uma.pt

Received 31 December 2023, revised 23 May 2024
Accepted for publication 4 July 2024
Published 15 July 2024

Abstract

The introduction of secondary ion-electron emission into an approximate model of non-equilibrium plasma layers on hot (thermionic) cathodes of high-pressure arc discharges allows extending the model to low cathode surface temperatures. Analysis of evaluation results shows that the extended model describes glow-like discharges on cold cathodes and thermionic arc discharges on hot cathodes, as it should. In the course of glow-to-arc transitions on cold cathodes, a transient regime occurs where a hot arc spot has just formed and a significant fraction of the current still flows to the cold surface outside the spot, so that the near-cathode voltage continues to be high. The power input in the near-cathode layer is very high in this regime, and so is the electron temperature in the near-cathode region. The mean free path for collisions between the atoms and the ions in these conditions exceeds the thickness of the layer where the ion current to the cathode is generated. A new method for evaluation of the ion current under such conditions is implemented. The developed model is applicable for cathode surface temperatures below the boiling point of the cathode material and may be used for multidimensional simulations of ignition of high-current arcs on refractory cathodes.

Keywords: arc discharges, arc electrodes, non-equilibrium arc plasmas, arc modeling

1. Introduction

Understanding the ignition of high-current arc discharges on cold cathodes in high-pressure gases is of significant theoretical and applied interest, in particular in view of the significant erosion of refractory cathodes of high-current arc discharges that occurs during ignition. Unfortunately, there are no self-consistent methods for numerical simulation of the ignition of high-current arcs on cold cathodes. The most difficult is the self-consistent description of the current transfer to the cathodes at the initial stage of arc ignition, when the cathode surface is not yet hot enough for thermionic emission.

Various hypotheses on the dominating mechanism of current transfer to the surfaces of cold arc cathodes have been proposed in the arc discharge literature: thermo-field electron emission from the cathode (e.g. review [1]), explosive/evaporative and field electron emission (e.g. book [2]), secondary

* Author to whom any correspondence should be addressed.

electron emission from impact of excited atoms [3], charge transport by ions coming to the cathode surface from the plasma (e.g. discussion in section 4 of review [4]). Another potentially important mechanism is secondary electron emission from ion impact, which is the dominating mechanism of current transfer to cold cathodes of low-current discharges such as glow and negative corona discharges.

In [5], the ignition of a high-current AC arc discharge on cold electrodes in atmospheric-pressure argon was investigated by means of the one-dimensional (1D) unified numerical modeling, with the aim to clarify the role of different mechanisms of current transfer to cold arc cathodes. It was found that, after a very brief (of the order of 0.1 μs) period of arcing time, when the displacement current is the dominating mechanism, the ion current comes into play and remains the dominating mechanism until the cathode is sufficiently hot for thermionic electron emission. The ionization energy, necessary for the generation of the ion current, is provided by work of the space-charge sheath electric field on secondary electrons emitted by the cathode surface under ion impact. No indications of explosive emission were found. Note that these results are consistent with those reported in [6] for 1D steady-state discharges in atmospheric-pressure nitrogen over a wide range of current densities, from 10^3 to $10^7\,\mathrm{A\,m^{-2}}$, obtained by means of 1D numerical modeling with account of a large number of neutral, excited, and charged plasma species.

The conclusion that the ion current and secondary electron emission from the cathode are the most important mechanisms of current transfer to cold cathodes of arc discharges was confirmed by specially designed experiments [7–9]. Thus, this conclusion has by now been substantiated both theoretically and experimentally and there appears to be no reason to doubt it.

The unified numerical modeling approach, used in [5, 6], is based on describing the plasma in the whole interelectrode gap by the single set of differential equations, comprising conservation and transport equations for each plasma species, the electron and heavy-particle energy equations, and the Poisson equation. These equations are solved jointly with the heat conduction and current continuity equations in the body of the electrodes. This approach does not rely on apriori assumptions, such as quasi-neutrality and thermal and/or chemical equilibrium in different regions of the arc, and is in this sense similar to the fluid modeling of cold gas discharges, which is well developed and universally used for simulations of, e.g. glow, radiofrequency, dielectric barrier, corona, and streamer discharges. When applicable, the unified modeling is in most situations the most comprehensive and reliable simulation approach for arc discharges.

The unified modeling approach has been successfully applied for axially symmetric modeling of low-current arc discharges [10–15]. Unfortunately, the approach is highly computationally intense for high values of the current density, and therefore its applications to high-current arcs are limited to one dimension in space; see citations in section 3.1 of [4] and [5, 6, 16–21] as further references. The arc-electrode interaction in geometries of practical interest is a multidimensional phenomenon. Consequently, the unified modeling approach is impractical for high-current arcs and approximate models, which are less intense numerically, are needed. Many references to approximate models of arc-electrode interaction can be found in reviews [4, 22]. In particular, there are models of non-equilibrium plasma layers on hot refractory, or thermionic, cathodes of high-pressure arc discharges [23–30]. Such models have been used for investigation of arc plasma interaction with thermionic cathodes and also as modules of multidimensional numerical codes describing the arc on the whole; e.g. review [4] and references therein.

The modeling of the ignition of a high-current AC arc discharge on cold electrodes [5] revealed a similarity between the physics of current transfer to cold and hot refractory cathodes: in both cases, there is a regime where the ion current to the cathode is limited not by a finite rate of diffusion of the ions from the non-equilibrium near-cathode plasma layer to the cathode surface, but rather by a finite rate of supply of the ionization energy to the near-cathode layer, which is provided by work of the space-charge sheath electric field on electrons emitted by the cathode surface. Therefore, one can attempt to extend approximate models of the interaction of high-pressure arcs with hot refractory (thermionic) cathodes, in order to make them applicable to both hot and cold cathodes, simply by introducing an account of secondary electron emission from ion impact, along with the thermionic electron emission. Of course, the success of such attempt is not guaranteed, in particular, since the integral-balance evaluation of the electron temperature in the near-cathode layer, which is typical of approximate models for thermionic cathodes and is reasonably accurate for partially to fully ionized plasma layers near hot cathode surfaces (e.g. section 3.4 of [4]), is not necessarily suitable for weakly ionized plasmas near cold cathodes. On the other hand, if such attempt is successful, the extended model will offer a simple tool for multidimensional modeling of the ignition of high-current arc discharges on cold refractory electrodes in conditions of practical interest.

Therefore, the question as to whether the extended model, obtained by introducing an account of secondary ion-electron emission into an approximate model of the interaction of high-pressure arcs with hot refractory cathodes, will be is at least qualitatively accurate for cold cathodes, is non-trivial and worthy of investigation. This question is addressed in this contribution. The treatment is limited to cathode surface temperatures below the boiling point of the cathode material, when the vaporization of the cathode material is not a dominating effect and the arc may be considered as burning in the ambient gas.

The outline of the paper is as follows. In section 2, a model of non-equilibrium arc plasma layers near thermionic cathodes is extended to account for secondary ion-electron emission and results of calculation are given and analyzed. It is found that the model describes glow-like discharge regimes on cold cathodes and thermionic arc discharge regimes on hot cathodes, as it should. In section 3, a refined evaluation is considered of the ion current to the cathode surface for conditions where a hot spot has just appeared on the cathode surface while the

near-cathode voltage is still high, which occur during glow-to-arc transitions. Concluding remarks are given in section 4. A brief description of the basis of approximate modeling of arc plasma interaction with thermionic cathodes in given in appendix for convenience.

2. The extended model

The key element of the approximate approach to modeling the interaction of arc plasmas with thermionic cathodes, which is summarized in appendix, is a model of non-equilibrium near-cathode plasma layer. It is in this model that an account of the secondary electron emission from ion impact should be introduced, in the hope of extending the approach to cold cathodes. In the simplest approximation, one can neglect the possible interaction of thermionic and secondary ion-electron emission mechanisms and estimate the density $j_{\rm em}$ of the total electron emission current as the sum:

$$j_{\rm em} = j_{\rm T} + \gamma j_{\rm i}, \tag{1}$$

where $j_{\rm T}$ is the density of emission current caused by high values of the cathode surface temperature and/or electric field directed to the cathode surface, γ is the so-called effective secondary emission coefficient, and $j_{\rm i}$ is the density of electric current transported to the cathode surface by the ions coming from the plasma.

In principle, $j_{\rm T}$ may be determined with account of field to thermo-field to thermionic electron emission mechanisms by means of evaluating the Murphy–Good formalism [31]. However, the modeling [5] has shown that, under conditions where the term $j_{\rm T}$ on the rhs of equation (1) is non-negligible, the thermionic emission mechanism is dominating and the Richardson–Schottky formula may be used. Let us assume that γ characterizes all mechanisms of secondary electron emission—due to bombardment by ions, excited particles, and photons, as is often done in the modeling of cold discharges; for example, section 4.7.2 of [32]. (Note, however, that the simulations [5] have shown that the electron emission from impact of excited atoms is insignificant under conditions considered, while the role of photoeffect is typically small except in the case of discharge ignition by short voltage pulses, with duration smaller than the time of ion drift.)

Let us consider results obtained in this way with the use of the model of non-equilibrium plasma layers on thermionic cathodes in high-pressure arc discharges summarized in [23]. The cathode is made of tungsten, the plasma-producing gas is atmospheric-pressure argon. j_T is determined by means of the Richardson-Schottky formula, values of the work function and the Richardson constant for the cathode are those given in the reference book [33] for a polycrystalline tungsten surface: 4.55 eV and $6\times10^5\,{\rm A\,m^{-2}\,K^{-2}}$, respectively. The secondary electron emission coefficient γ equals 0.1.

The density of electric current from the plasma to the cathode surface in the extended model is evaluated as

$$j_{\rm c} = j_{\rm T} + (1+\gamma) j_{\rm i} - j_{\rm CD}, \tag{2}$$

where $j_{\rm CD}$ is the density of current of fast plasma electrons counter-diffusing to the cathode surface against the sheath electric field. The quantities involved in this expression are shown in figure 1 as functions of $T_{\rm c}$ the cathode surface temperature and U the near-cathode voltage drop, in agreement with what is described in appendix. Also shown is the electron temperature in the near-cathode layer, $T_{\rm e}$. The upper boundary of the range of $T_{\rm c}$, shown in each of the figures (a)–(d), is the same: 5000 K, in order to cover the entire temperature range of thermionic cathodes. The lower boundary for each voltage is chosen in a way that j_c is no smaller than $10^3\,{\rm A\,m^{-2}}$. For the voltages of 10 and 60 V, this happens for $T_{\rm c}$ exceeding approximately 2250 K. For the voltage of 157 and 200 V, $j_{\rm c}$ exceeds $10^3\,{\rm A\,m^{-2}}$ for all values of $T_{\rm c}$ down to room temperatures.

Also shown in figure 1 is parameter α, which is defined as

$$\alpha = \left[\frac{8}{3}\frac{\bar{Q}_{ia}^{(1,1)}}{k_i}\sqrt{\frac{kT_h}{\pi m_a}}\right]^{1/2}, \tag{3}$$

where $\bar{Q}_{ia}^{(1,1)}$ is the energy-averaged cross section for momentum transfer in ion-atom collisions, $k_i = k_i(T_e)$ is the rate constant of ionization of neutral atoms by electron impact, $T_{\rm h}$ is the heavy-particle temperature in the near-cathode layer (it is assumed that $T_{\rm h} = T_{\rm c}$), and m_a is the atom mass. Note that α defined in this way characterizes the ratio of the scale of thickness of the ionization layer, which is the outer section of the non-equilibrium near-cathode layer where the ion current to the cathode is generated, to the mean free path for collisions between the ions and the atoms [34].

In order to understand the results shown in figure 1, it is useful to consider the integral balance of electron energy in the ionization layer in the extended model. The power input into the electron gas is provided mainly by the acceleration of the emitted electrons by the electric field in the near-cathode layer and may be roughly estimated as $j_{\rm em}U$. A part of this power is spent on ionization inside the near-cathode layer and the rest is transported by the electron current into the bulk plasma:

$$j_{\rm em}U = \frac{j_{\rm i}}{e}A_{\rm i} + q, \tag{4}$$

where A_i is the ionization energy of the plasma-producing gas, e is the electron charge, and q is the density of flux of electron energy from the ionization layer into the bulk plasma, transported by the electron current. Note that the equation of integral balance of electron energy in the ionization layer could be written in a more detailed form (cf equation (14) of [23]), however the simple form (4) is appropriate for qualitative analysis.

With the use of equation (1), equation (4) may be rewritten as

$$j_{\rm T}U = j_{\rm i}C_1U + q, \tag{5}$$

where $C_1 = A_{\rm i}/eU - \gamma$.

Assume that the cathode surface temperature $T_{\rm c}$ increases at a fixed value of U. Let us first consider the case where U is smaller than $A_{\rm i}/e\gamma$ and hence $C_1 > 0$. (Since ionization energy

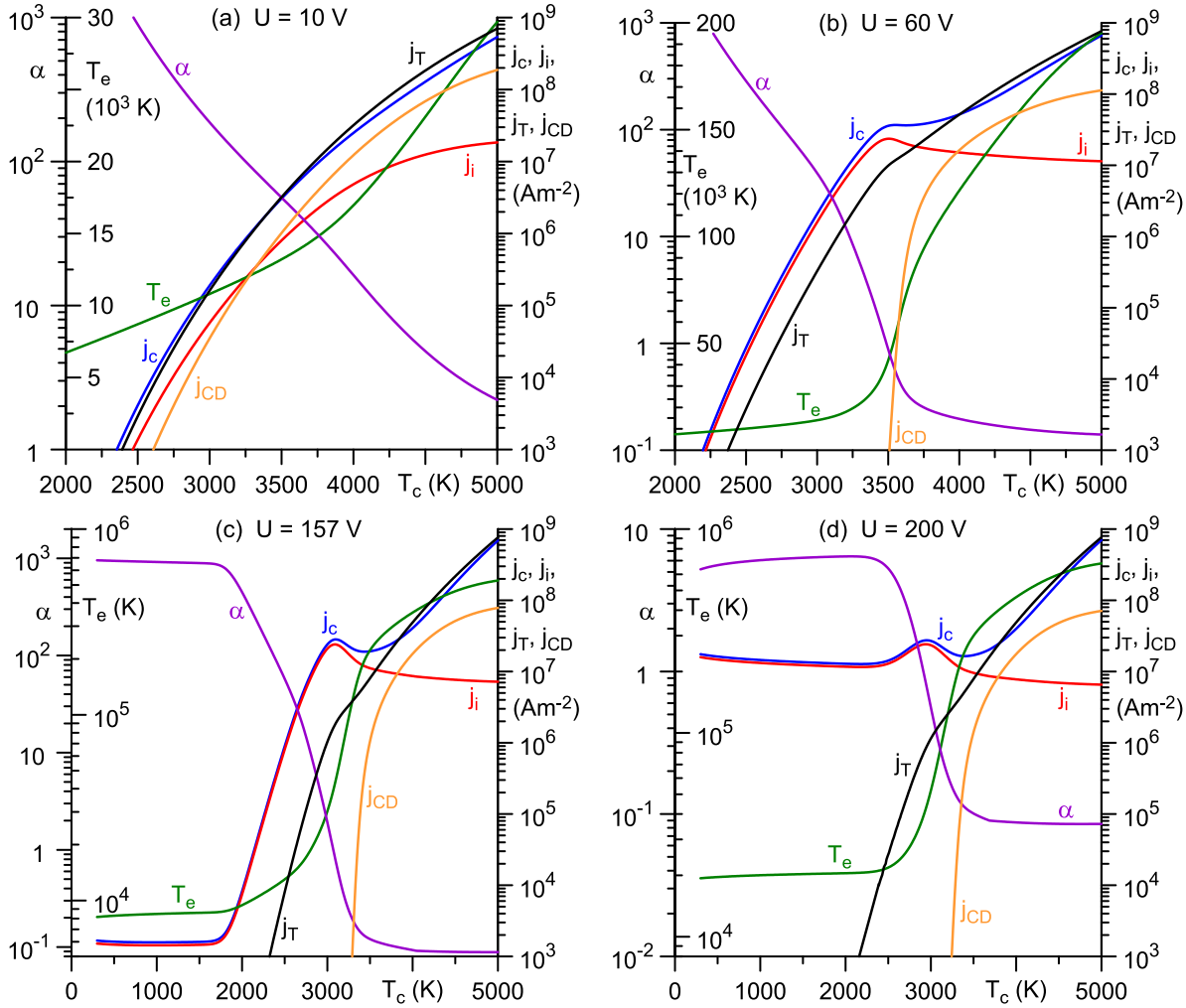

Figure 1. Characteristics of the non-equilibrium near-cathode plasma layer on a tungsten cathode in atmospheric-pressure argon arc.

of argon is 15.76 eV, $A_\mathrm{i}/e\gamma = 157.6$ V in the conditions considered.) For low and moderate values of T_c, when the thermionic emission current j_T and, consequently, the power input due to thermionic emission, $j_\mathrm{T}U$, are not high, the electron temperature in the ionization layer is not high as well and transport of the electron energy into the bulk is insignificant. Discarding the second term on the rhs of equation (5), one finds $j_\mathrm{i} \approx j_\mathrm{T}/C_1$. Thus, the ion current density is roughly proportional to the thermionic emission current density. In this regime, the ion current to the cathode is limited not by a finite rate of diffusion of the ions from the ionization layer to the cathode surface, but rather by a finite rate of supply of the ionization energy to the ionization layer. This regime occurs on thermionic arc cathodes when they are not hot enough for the plasma in the near-cathode layer to attain full ionization.

As T_c increases, the power input $j_\mathrm{T}U$ and the electron temperature in the ionization layer, T_e, increase as well and the ionization degree of the plasma also increases. As the plasma at the edge of the ionization layer approaches full ionization, the ion current j_i becomes saturated and the term $j_\mathrm{i}C_1U$ cannot compensate the power input $j_\mathrm{T}U$, meaning that the second term on the rhs of equation (5) comes into play and j_i is no longer proportional to j_T.

In the case where U is close to $A_\mathrm{i}/e\gamma$ (and $|C_1|$ is small), the ion current can be significant even for low cathode surface temperatures, when j_T is negligible. In other words, the secondary electron emission is strong enough to supply the necessary ionization energy to the near-cathode plasma; the glow discharge regime. The dependence of j_i on T_c is weak in this regime.

The glow discharge regime occurs also in the case where U exceeds $A_\mathrm{i}/e\gamma$ ($C_1 < 0$). The plasma at the edge of the ionization layer is strongly to fully ionized for all values of T_c.

Taking into account that C_1 approximately equals 1.5 for $U = 10$ V and 0.16 for $U = 60$ V, one can conclude that the above reasoning explains the behavior of the dependence of the ion current density j_i on the cathode surface temperature T_c seen in figures 1(a) and (b). The cathode operates in the thermionic regime. The glow discharge regime with a virtually constant j_i occurs in the range $T_\mathrm{c} \lesssim 1700$ K for $U = 157$ V, as seen in figure 1(c), and a thermionic arc cathode regime with j_i increasing more or less proportionally to j_T occurs for higher

T_c (note that $C_1 \approx 4 \times 10^{-4}$ for $U = 157$ V). For $U = 200$ V, the glow discharge regime with a virtually constant j_i occurs in the range $T_c \lesssim 2200$ K as seen in figure 1(d).

As discussed above, an increase in the power input in the ionization layer, $j_T U$, causes an increase in the electron temperature in the ionization layer, T_e. This effect is clearly seen in figure 1 in the range of cathode surface temperatures higher than approximately 2250 K, where the thermionic emission current j_T comes into play. Understandably, the effect is particularly strong for higher U: values of T_e in excess of 10^5 K are seen in figures 1(b)–(d). This effect is very interesting and one could explore the possibility of its experimental verification; this point is discussed in some detail below.

The maximum in the dependence $j_i(T_c)$ occurs for T_c approximately equal to 3500 K for $U = 60$ V, to 3100 K for 157 V, and to 2940 K for 200 V). It is seen in figures 1(b)–(d) that the plasma at the edge of the ionization layer is already fully ionized under these conditions (atmospheric-pressure argon plasma approaches full ionization as the electron temperature reaches values around 20 000 K), again in agreement with the above reasoning. After the maximum, the dependence $j_i(T_c)$ monotonically decreases. For $U = 157$ and 200 V, this causes a decrease in j_c the density of the net electric current to the cathode surface in the range of T_c from approximately 3000–3500 K, as seen in figures 1(c) and (d); an effect that at first glance seems nontrivial.

The decrease of the density of ion current to the cathode surface with increasing surface temperature at a high fixed near-cathode voltage drop is unrelated to the account of the secondary electron emission, introduced in this work, and is present also in the original model [23]. The density of the ion current in the model [23] is evaluated as

$$j_i = e n_i^{(0)} v_s f_w. \tag{6}$$

Here $n_i^{(0)}$ is the charged particle density at the 'edge' of the ionization layer, estimated from the Saha equation in terms of the plasma pressure and the electron and heavy-particle temperatures; $v_s = \sqrt{k(T_h + T_e)/m_a}$ is the Bohm speed; and f_w is the normalized ion current density, which depends, in particular, on α and is given by equation (11) of [23]. Note that the latter equation combines the diffusion description of the relative motion of the ions and the atoms in the ionization layer for $\alpha \gtrsim 1$ and a more sophisticated multifluid treatment for $\alpha \lesssim 1$, when the mean free path for collisions between the atom and the ions is comparable to or larger than the thickness of the ionization layer and the diffusion description of the relative motion of the ions and the atoms is inapplicable. It is seen from figures 1(b)–(d) that α is of the order unity or smaller under conditions where the decreasing dependence $j_i(T_c)$ occurs, so the multifluid description comes into play under these conditions.

When the plasma at the edge of the ionization layer is fully ionized, the charged particle density $n_i^{(0)}$ at constant pressure decreases with increasing T_c in inverse proportion to $(T_c + T_e)$. The product $n_i^{(0)} v_s$ decreases in inverse proportion to $\sqrt{T_c + T_e}$. It is seen from figures 1(a)–(d) that α decreases with increasing T_c. Since f_w in the multifluid theory decreases with decreasing α in the range $\alpha \lesssim 1$, it follows from equation (6) that j_i decreases as well. This explains the decrease in the dependence $j_i(T_c)$, seen in in figures 1(b)–(d) for T_c exceeding approximately 3000–3500 K.

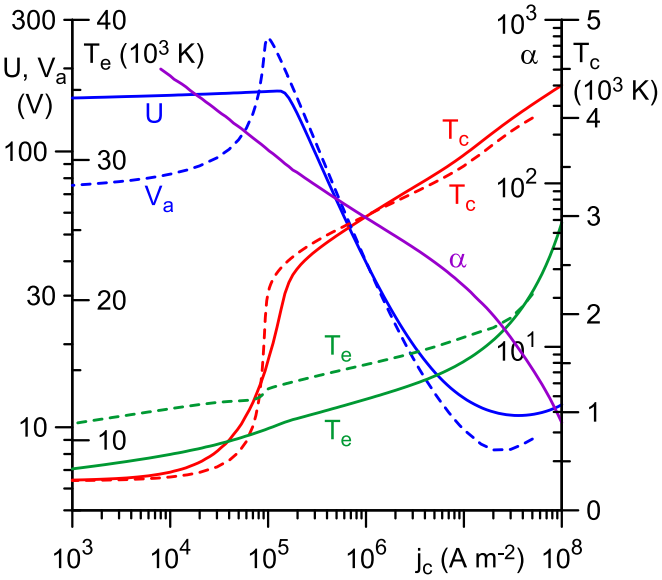

Figure 2. Characteristics of the cathodic part of a steady-state arc on a 1 cm-high tungsten cathode in atmospheric-pressure argon. Solid: approximate modeling with the use of the extended model. Dashed: unified modeling [5].

A comparison of results given by the approximate and unified models is shown in figure 2, which refers to a steady-state arc on a 1 cm-high rod tungsten cathode in atmospheric-pressure argon. The temperature of the cathode base is 293 K. For simplicity, the densities of the electric current and the energy flux from the plasma to the lateral surface of the cathode are discarded; in other words, the lateral surface of the cathode is assumed to be electrically and thermally insulated. Then the temperature distribution inside the cathode is 1D and the temperature and the current density at all points of the current-collecting front surface of the cathode are the same.

The solid lines in figure 2 depict characteristics of the cathodic part of the arc, obtained by performing the second step of the approximate modeling procedure, described in appendix, with the use of the extended model of non-equilibrium plasma layers on arc cathodes considered in this section. Note that the cathode surface temperature T_c in this modeling is not a control parameter but rather a modeling result, in contrast to the computation of the characteristics of the near-cathode layer shown in figure 1. The only control parameter in the modeling shown in figure 2 is the near-cathode voltage U. Performing calculations for various values of U, one computes the current–voltage characteristic of the near-cathode region, $j_c(U)$. This characteristic is shown in figure 2 in the form $U(j_c)$. Also shown are the dependences $T_c(j_c)$, $T_e(j_c)$, and $\alpha(j_c)$.

The dashed lines in figure 2 represent characteristics of the arc obtained with the use of the unified model [5]. The

computation domain in this case included 1 cm-high tungsten cathode, 1 cm-high tungsten anode, and a 1 mm-long arc. The electron temperature T_e shown by the dashed line was evaluated in the unified model at an 'edge' of the space-charge sheath, defined as a point where the charge separation is 10%. There is a good agreement between the dependences $T_c(j_c)$ and $T_e(j_c)$ given by the two models. Values of the near-cathode voltage in the approximate model, $U(j_c)$, and of the arc voltage in the unified model, $V_a(j_c)$, are rather close to each other for current densities exceeding approximately $2\times10^5\,\mathrm{A\,m^{-2}}$. For lower j_c, the difference is bigger, although the qualitative agreement is preserved. Note that the relative motion of the ions and the atoms in the ionization layer is described in the two models in different ways: the diffusion description is used in the unified model, while the approximate model employs the diffusion description for $\alpha \gtrsim 1$ and the multifluid theory for $\alpha \lesssim 1$. However, this difference is irrelevant under conditions of figure 2 since α exceeds unity for all j_c, and the agreement between the approximate and unified models is not surprising.

One can conclude that the introduction of secondary electron emission into the approximate model of non-equilibrium near-cathode plasma layers on thermionic cathodes of high-pressure arc discharges [23] allows one to extend the model, in a qualitatively correct way, to cold cathodes and thus to obtain a self-consistent description of glow-like discharge regimes on cold cathodes and thermionic arc discharge regimes on hot cathodes.

3. Refined evaluation of the ion current to the cathode during glow-to-arc transitions

There is another theoretical aspect that requires attention as far as glow-to-arc transitions on cold cathodes are concerned: the description of the relative motion of the ions and the atoms in the ionization layer.

The approach to numerical modeling of high-pressure arc plasma interaction with hot thermionic cathodes, based on the model of non-equilibrium near-cathode layers [23], has been tested experimentally over a wide range of conditions of hot cathodes, and this may be considered as an indirect experimental verification of the model. However, one should keep in mind that the parameter α exceeds unity for hot cathodes, which is due to low near-cathode voltages on hot cathodes. An example is seen in figure 2: in the range $j_c \gtrsim 10^6\,\mathrm{A\,m^{-2}}$, where the cathode surface temperature increases from 3000 to above 4000 K, the near-cathode voltage U falls approximately from 40 to 10 V, and $\alpha > 1$ under such conditions. Therefore, the above-mentioned indirect experimental verification of the model [23] refers to conditions with $\alpha > 1$, where the relative motion of the ions and the atoms is adequately described by the diffusion approximation. The model remains untested for cases where $\alpha \lesssim 1$ and the multifluid description becomes relevant.

On the other hand, cases where both T_c and U are high and, consequently, $\alpha \lesssim 1$, do occur in regimes intermediate between the glow and arc regimes, where a hot arc spot is just formed and a significant fraction of the current still flows to the cold surface outside the spot, so that the near-cathode voltage remains high at all points of the cathode surface, including in the spot. Let us consider, as an example, results of numerical simulations [14], performed for a steady-state (DC) discharge on a 1.5 mm-radius W cathode in 1 atm Ar in the range of discharge currents I up to 20 A. A stationary state with a discharge voltage of 60 V and a narrow spot on the cathode with the temperature of 3960 K was found for $I = 2.5$ A. One can see from figure 1(b) that α is around 0.2 for such conditions. (It is worth noting that the ratio of the mean free path for collisions between the atoms and the ions to the scale of thickness of the ionization layer, estimated for this α value with the use of formulas [34], is about 50.) Transient states with similar characteristics were encountered in time-dependent numerical simulations of ignition of a 200 A atmospheric-pressure Ar arc on a W insert with conical tip, surrounded by a water-cooled copper holder [35], and on a W rod-like cathode [36].

Thus, in order to develop a reliable method of simulation of ignition of high-pressure arcs on cold refractory cathodes, it might be helpful to revisit the description of the relative motion of the ions and the atoms in the ionization layer for $\alpha \lesssim 1$ and to check whether the multifluid treatment needs to be refined. Another relevant question is whether the decreasing dependence $j_c(T_c)$ for high U and T_c, seen in figures 1(c) and (d) in the range $3000\,\mathrm{K} \lesssim T_c \lesssim 3500\,\mathrm{K}$, will remain if the evaluation of the ion current for $\alpha \lesssim 1$ is refined.

A refined theory of the ionization layer in partially to fully ionized high-pressure arc plasma was developed in [34]. A fluid description of the ion species in the ionization layer was combined with a kinetic description of the atom species. The following formula was obtained for the density of ion current to the cathode:

$$f_w = \frac{C_2 C_3}{C_2 + C_3\alpha}, \tag{7}$$

where C_2 is the dimensionless coefficient defined by equation (14) of [37], which varies between approximately 0.67 and 1, and $C_3 = \{2 - \sqrt{2/[\pi(1+T_e/T_h)]}\}^{-1}$. It was found that equation (7) conforms to experiment better than the multifluid theory, although the scatter of the available experimental data is too great to make an unambiguous conclusion.

Switching in the near-cathode plasma layer model [23] from the multifluid description of the ionization layer to the hybrid description [34] amounts to replacing equation (11) of [23] with equation (7). The effect of this switching is illustrated by figure 3. The ion current in the region where $\alpha \lesssim 1$ becomes higher, however the dependence $j_i(T_c)$ remains decreasing. The dependence $j_c(T_c)$ remains non-monotonic in the range of T_c between approximately 3100 and 3500 K, although the non-monotony becomes less pronounced.

The function f_w described by equation (7) increases with decreasing α. However, α does not change much at high T_c, as seen from figure 3, therefore the increase in f_w with increasing T_c is weak and insufficient to compensate the decrease in $n_i^{(0)} v_s$ for conditions where the plasma is fully ionized. Hence,

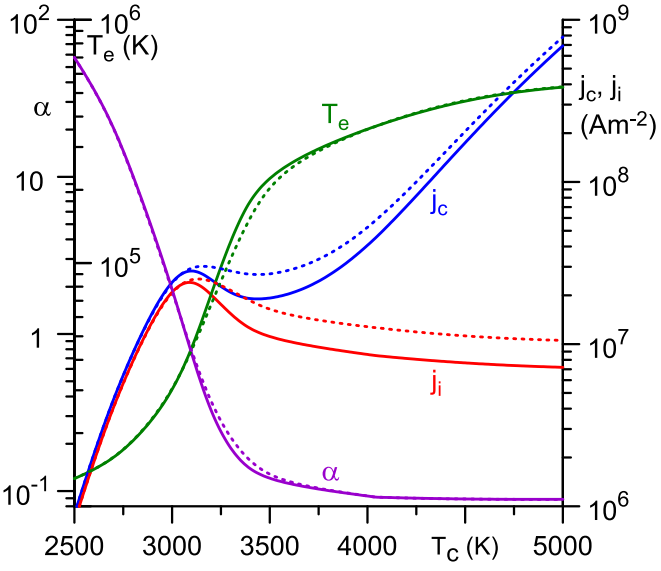

Figure 3. Characteristics of the nonequilibrium near-cathode plasma layer on a tungsten cathode in an atmospheric-pressure argon arc. $U = 157$ V. Solid: the extended model described in section 2. Dotted: the extended model employing equation (7).

the rhs of equation (6) is decreasing with increasing T_c, which explains the decrease in the dependence $j_i\,(T_c)$, seen in figure 3 for $T_c \gtrsim 3100$ K.

Thus, changing the description of the relative motion of the ions and the atoms in the ionization layer from multifluid to hybrid has led to a relatively weak change in integral characteristics of the near-cathode layer.

4. Conclusions

The introduction of secondary electron emission into an approximate model of non-equilibrium plasma layers on hot (thermionic) cathodes of high-pressure arc discharges allows extending the model to low cathode surface temperatures. The extended model describes glow-like discharge modes on cold cathodes and thermionic arc discharge modes on hot cathodes. This is an essential step in developing practicable self-consistent modeling methods for multidimensional simulation of ignition of high-current arcs on cold refractory cathodes and for evaluation of the erosion of refractory cathodes that occurs during arc ignition.

In the course of glow-to-arc transitions on cold cathodes, a transient regime occurs where a hot arc spot has just formed and a significant fraction of the current still flows to the cold surface outside the spot, so that the near-cathode voltage continues to be high at all points of the cathode surface, including in the spot. The power input in the ionization layer, $j_T U$, is very high in this regime. Therefore, one should expect that the electron temperature is very high as well, as seen in figures 1(b)–(d). Indeed, first results of the modeling of the ignition of 200 A arcs on cold tungsten cathodes of different configurations [35, 36], performed with the use of the extended model, indicated that the electron temperature in the near-cathode layer reaches values of the order of 10^5 K.

The thickness of the ionization layer, where the ion current to the cathode is generated, under such conditions becomes comparable to, or smaller than, the mean free path for collisions between the atoms and the ions. The introduction into the extended model of the hybrid theory [34], combining a fluid description of the ion motion in the ionization layer with a kinetic description of the atom motion, leads to prediction of higher ion current densities for cathode surface temperatures exceeding approximately 3000 K. However, the dependence of the density of current to the cathode surface on the surface temperature at a high fixed near-cathode voltage drop remains non-monotonic, although the non-monotony becomes less pronounced.

If the electron temperature in the near-cathode layer briefly becomes very high in the course of the high-current arc ignition on a cold cathode, as predicted by the extended model, then the electron temperature in the plasma ball adjacent to the newly-formed cathode arc spot briefly becomes very high as well. It is of interest to simulate the distribution of the electron temperature in the plasma ball, in order to explore the possibility of experimental verification of this conclusion. This will require multidimensional two-temperature MHD modeling of the arc plasma beyond the thin non-equilibrium near-cathode layer, and the extended model will provide boundary conditions for this modeling.

Data availability statement

All data that support the findings of this study are included within the article (and any supplementary files).

Acknowledgments

The work was supported by FCT—Fundação para a Ciência e a Tecnologia of Portugal under Projects UIDB/50010/2020 (https://doi.org/10.54499/UIDB/50010/2020), UIDP/50010/2020 (https://doi.org/10.54499/UIDP/50010/2020), LA/P/0061/2020 (https://doi.org/10.54499/LA/P/0061/2020) and by European Regional Development Fund through the Operational Program of the Autonomous Region of Madeira 2014–2020 under Project PlasMa-M1420-01-0145-FEDER-000016.

Appendix. Summary of approximate modeling of arc plasma interaction with thermionic cathodes

The dominating mechanism of current transfer to hot (thermionic) arc cathodes is thermionic electron emission from the cathode; contribution of the ion current from the plasma is typically ten to twenty percent. Nevertheless, the role of the ion current is indispensable: it is the ion bombardment that heats the cathode surface to high temperatures necessary for thermionic emission.

Available approximate models of arc plasma interaction with thermionic cathodes refer to the case where the arc bulk is in the state of ionization (Saha) equilibrium, which is a typical case for high-current high-pressure arcs as shown, e.g. by estimates of section 2.2 of [4]. A thin region near the cathode surface where deviations from ionization equilibrium are localized may be called near-cathode non-equilibrium plasma layer. The plasma in the outer section of this layer is quasi-neutral. It is in this section, which is called ionization layer, that the ion current to the cathode surface is formed. The ionization layer is separated from the cathode surface by a still thinner layer where space charge is localized; the space-charge sheath.

Ions generated in the ionization layer move across the space-charge sheath, where they are accelerated by the sheath electric field, to the cathode surface, where they recombine. Neutral atoms thus formed are desorbed from the surface and move into the plasma, with some or all of them being ionized upon reaching the ionization layer. Electrons emitted by the cathode surface are accelerated by the electric field when crossing the space-charge sheath and ionize neutral atoms when crossing the ionization layer. Work of the sheath electric field on the emitted electrons is the main source of the ionization energy.

For work of the sheath electric field on the emitted electrons to be sufficient to provide the ion current required, the sheath voltage has to be on the order of 10 V or higher. Therefore, a significant power is deposited by the arc power supply into the near-cathode layer. Consequently, the operation of the cathodic part (the cathode and the near-cathode non-equilibrium plasma layer) of a high-pressure arc discharge with a thermionic cathode is dominated by processes in the near-cathode non-equilibrium plasma layer and is virtually unaffected by processes in the arc bulk; e.g. section 3.3.1 of [4].

This allows one to decouple the calculation of the cathodic part from the rest of the arc. This is done in two steps. First, one solves 1D equations describing the near-cathode non-equilibrium plasma layer and finds all parameters of the layer, in particular, the densities of energy flux and electric current from the plasma to the cathode surface, q_c and j_c, as functions of the local cathode surface temperature T_c and the near-cathode voltage drop U: $q_c = q_c(T_c, U), j_c = j_c(T_c, U)$. A model of non-equilibrium near-cathode plasma layers in high-pressure arc discharges is needed to perform these calculations. Several such models have been developed for thermionic cathodes [23–30].

At the second step, one solves the multidimensional equation of heat conduction in the cathode body. If Joule heat production in the cathode body can play a role, this equation should be coupled with the current continuity equation. The boundary conditions at the cathode surface are $\kappa_s \partial T_s/\partial n = q_c(T_c, U)$, $\sigma_s \partial \varphi_s/\partial n = j_c(T_c, U)$, where T_s and φ_s are the temperature and potential distributions inside the cathode, κ_s and σ_s are thermal and electric conductivities of the cathode material, and n is a direction locally orthogonal to the cathode surface and directed into the plasma. In the first approximation, this problem can be solved neglecting variations in the near-cathode voltage drop U along the cathode surface, caused by the electrical resistance of the adjacent part of the bulk; these variations are usually not significant and may be readily taken into account if needed. After this problem has been solved for a given U, one will know distributions along the surface of the temperature and, consequently, all the other parameters including j_c, corresponding to the U value being considered. These distributions may be used as boundary conditions for MHD modeling of the arc column. The arc current corresponding to the considered U will be known as well. Then the problem is solved for another U value *etc*.

Note that hot thermionic cathodes are widely used for primary electron production in plasma sources, both at high and low pressures; e.g. recent work [38] and references therein. In some cases, the physics of the interaction of emissive cathodes with the plasma is substantially different from that in high-pressure arc discharges. For example, such is the case of the so-called inverse sheaths; e.g. [39–41]. On the other hand, there are cases where the physics is similar to some extent. For example, this is the case of an emissive tungsten cathode immersed in a magnetized plasma column, which was investigated experimentally and numerically in [38]. The approximate models of plasma-cathode in high-pressure arc discharges, considered here, may be useful in such cases.

ORCID iDs

D F N Santos https://orcid.org/0000-0002-2377-766X
N A Almeida https://orcid.org/0000-0002-6499-3609
M S Benilov https://orcid.org/0000-0001-9059-1948

References

[1] Murphy A B 2015 *Plasma Chem. Plasma Process.* **35** 471
[2] Boulos M I, Fauchais P and Pfender E 2016 *Handbook of Thermal Plasmas* (Springer)
[3] Lowke J J, Murphy A B and Tanaka M 2019 *J. Phys. D: Appl. Phys.* **52** 444004
[4] Benilov M S 2020 *J. Phys. D: Appl. Phys.* **53** 013002
[5] Santos D F N, Lisnyak M, Almeida N A, Benilova L G and Benilov M S 2021 *J. Phys. D: Appl. Phys.* **54** 195202
[6] Saifutdinov A I 2021 *J. Appl. Phys.* **129** 093302
[7] Frohnert S and Mentel J 2022 *Contrib. Plasma Phys.* **62** e202100212
[8] Frohnert S and Mentel J 2022 *Contrib. Plasma Phys.* **62** e202100214
[9] Frohnert S and Mentel J 2022 *Contrib. Plasma Phys.* **62** e202100216
[10] Kolev S and Bogaerts A 2015 *Plasma Sources Sci. Technol.* **24** 015025
[11] Saifutdinov A I, Fairushin I I and Kashapov N F 2016 *JETP Lett.* **104** 180
[12] Kolev S, Sun S, Trenchev G, Wang W, Wang H and Bogaerts A 2017 *Plasma Process. Polym.* **14** 1600110
[13] Baeva M, Uhrlandt D and Loffhagen D 2020 *Jpn. J. Appl. Phys.* **59** SHHC05
[14] Saifutdinov A I 2022 *Plasma Sources Sci. Technol.* **31** 094008
[15] Tsonev I, Boothroyd J, Kolev S and Bogaerts A 2023 *Plasma Sources Sci. Technol.* **32** 054002
[16] Baeva M, Loffhagen D, Becker M M and Uhrlandt D 2019 *Plasma Chem. Plasma Process.* **39** 949
[17] Baeva M, Loffhagen D and Uhrlandt D 2019 *Plasma Chem. Plasma Process.* **39** 1359

[18] Baeva M, Methling R and Uhrlandt D 2021 *Plasma Phys. Technol.* **8** 1
[19] Baeva M, Stankov M, Trautvetter T, Methling R, Hempel F, Loffhagen D and Foest R 2021 *J. Phys. D: Appl. Phys.* **54** 355205
[20] Santos D F N, Almeida N A, Lisnyak M, Gonnet J-P and Benilov M S 2022 *Phys. Plasmas* **29** 043503
[21] Baeva M, Benilov M S, Zhu T, Testrich H, Kewitz T and Foest R 2022 *J. Phys. D: Appl. Phys.* **55** 365202
[22] Choquet I 2018 *Weld. World* **62** 177
[23] Benilov M S, Cunha M D and Naidis G V 2005 *Plasma Sources Sci. Technol.* **14** 517
[24] Wendelstorf J 1999 *Contributed Papers of 24th Int. Conf. on Phenomena in Ionized Gases, Warsaw 1999* vol 2, ed P Pisarczyk, T Pisarczyk and J Wolowski (Institute of Plasma Physics and Laser Microfusion) pp 227–8
[25] Schmitz H and Riemann K-U 2002 *J. Phys. D: Appl. Phys.* **35** 1727
[26] Lichtenberg S, Dabringhausen L, Langenscheidt O and Mentel J 2005 *J. Phys. D: Appl. Phys.* **38** 3112
[27] Scharf F H, Langenscheidt O and Mentel J 2007 *Proc. 28th ICPIG (Prague, July 2007)* ed J Schmidt, M Šimek, S Pekárek and V Prukner (Institute of Plasma Physics AS CR) pp 1252–5
[28] Sun Q, Wang C, Chen T and Xia W-D 2017 *J. Phys. D: Appl. Phys.* **50** 425202
[29] Mohsni C, Baeva M, Franke S, Gortschakow S, Gonzalez D, Araoud Z and Charrada K 2019 *Plasma Phys. Technol.* **6** 51
[30] Mohsni C, Baeva M, Franke S, Gortschakow S, Araoud Z and Charrada K 2020 *Phys. Plasmas* **27** 073514
[31] Murphy E L and Good R H 1956 *Phys. Rev.* **102** 1464
[32] Raizer Y P 1991 *Gas Discharge Physics* (Springer)
[33] Gale W F and Totemeier T C (eds) 2004 *Smithells Metals Reference Book* 8th edn (Elsevier Butterworth-Heinemann)
[34] Benilov M S 2024 *Plasma Sources Sci. Technol.* **33** 055002
[35] Cunha M D, Sargsyan M A, Gadzhiev M K, Tereshonok D V and Benilov M S 2023 *J. Phys. D: Appl. Phys.* **56** 395204
[36] Ojeda O, Cressault Y, Teulet P, Gonnet J-P, Santos D F N, Cunha M D and Benilov M S 2023 *23rd Int. Conf. Gas Discharges and Their Applications* vol 1 pp 64–67
[37] Benilov M S 1999 *J. Phys. D: Appl. Phys.* **32** 257
[38] Pagaud F, Dolique V, Claire N and Plihon N 2023 *Plasma Sources Sci. Technol.* **32** 115019
[39] Campanell M D 2013 *Phys. Rev.* E **88** 033103
[40] Taccogna F 2014 *Eur. Phys. J.* D **68** 199
[41] Zhang Z, Wu B, Yang S, Zhang Y, Chen D, Fan M and Jiang W 2018 *Plasma Sources Sci. Technol.* **27** 06LT01